JACS
JOURNAL OF THE AMERICAN CHEMICAL SOCIETY
pubs.acs.org/JACS
Article

An ROS-Responsive Donor That Self-Reports Its H_2S Delivery by Forming a Benzoxazole-Based Fluorophore

Qiwei Hu, Changlei Zhu, Rynne A. Hankins, Allison R. Murmello, Glen S. Marrs, and John C. Lukesh, III*

Cite This: J. Am. Chem. Soc. 2023, 145, 25486−25494
Read Online
ACCESS | Metrics & More | Article Recommendations | Supporting Information

ABSTRACT: Hydrogen sulfide (H_2S), an endogenous signaling molecule, is known to play a pivotal role in neuroprotection, vasodilation, and hormonal regulation. To further explore the biological effects of H_2S, refined donors that facilitate its biological delivery, especially under specific (patho) physiological conditions, are needed. In the present study, we demonstrate that *ortho*-substituted, aryl boronate esters provide two unique and distinct pathways for H_2S release from thioamide-based donors: Lewis acid-facilitated hydrolysis and reactive oxygen species (ROS)-induced oxidation/cyclization. Through a detailed structure−activity relationship study, donors that resist hydrolysis and release H_2S solely via the latter mechanism were identified, which have the added benefit of providing a potentially useful heterocycle as the lone byproduct of this novel chemistry. To highlight this, we developed an ROS-activated donor (**QH642**) that simultaneously synthesizes a benzoxazole-based fluorophore en route to its H_2S delivery. A distinct advantage of this design over earlier self-reporting donors is that fluorophore formation is possible only if H_2S has been discharged from the donor. This key feature eliminates the potential for false positives and provides a more accurate depiction of reaction progress and donor delivery of H_2S, including in complex cellular environments.

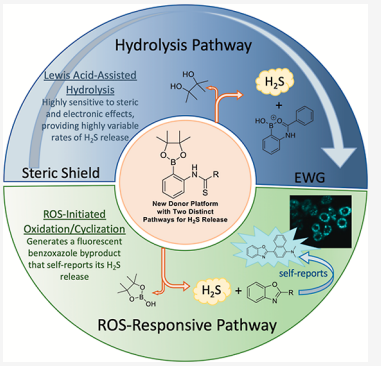

INTRODUCTION

Gasotransmitters are endogenous signaling molecules that, similar to hormones and neurotransmitters, elicit important physiological and pathophysiological effects within the human body that stem from their action at specific cellular targets.[1−3] In addition to nitric oxide (NO) and carbon monoxide (CO), hydrogen sulfide (H_2S) is the most recently recognized member among this select group of gaseous signaling molecules.[4−8]

H_2S is endogenously produced in small amounts in mammals primarily via the enzymatic desulfhydration of cysteine and homocysteine.[9−11] Enzymatic regulation provides strict control over its biosynthesis and ensuing biological effects, which include neuroprotection,[12] vascular relaxation,[13,14] hormonal regulation,[15] and energy production.[16] Given this activity, it comes as no surprise that exogenous H_2S supplementation is being explored with great interest in preclinical models of human illnesses, including neurological disorders such as Parkinson's and Alzheimer's disease,[17−19] cardiovascular-related pathologies,[20−26] and other age-related illnesses.[27,28]

Traditional methods for delivering H_2S to biological systems include the use of sulfide salts (NaHS and Na_2S) as convenient, H_2S equivalents in buffer. Their use, however, results in a bolus effect that poorly mimics the natural enzymatic production of H_2S and often leads to toxic, adverse effects.[29,30] For these reasons, synthetic donors, or H_2S releasing compounds, were sought in an effort to provide the prolonged delivery of H_2S at concentrations that are therapeutically relevant.

A water-soluble derivative of Lawesson's reagent, named GYY4137, was the first example of a synthetic H_2S donor developed for this purpose.[31] While GYY4137 has displayed promising therapeutic potential in several disease models, its inefficiency and lack of spatiotemporal control over its H_2S delivery have led to a search for more efficient, stimulus-responsive donors whose activation can be more easily tuned to specific biological conditions.[32−36]

To assist in these efforts, we recently developed a new and general design strategy for improving the selectivity and efficiency of H_2S release from thioamide-based donors by enlisting intramolecular nucleophilic assistance, initiated by a precise biological stimulus (Scheme 1).[37] In our initial study, we demonstrated that both disulfide- and diselenide-linked thioamides were responsive to biologically relevant concentrations of glutathione and released H_2S in high yield and through a well-defined mechanistic pathway that provided an

Received: September 21, 2023
Revised: October 24, 2023
Accepted: November 1, 2023
Published: November 11, 2023

https://doi.org/10.1021/jacs.3c10446
J. Am. Chem. Soc. 2023, 145, 25486−25494

Scheme 1. General Design Strategy for Increasing the Rate, Efficiency, and Selectivity of H_2S Release from Thioamide-Based Donors, Previously Reported by Our Group

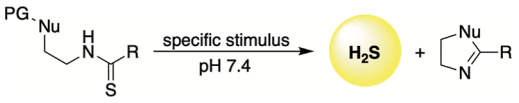

easily identifiable byproduct (control compound for biological studies). Moreover, we observed that diselenide-based donors appeared to afford more selectivity and control over their H_2S release as they required significantly stronger reducing conditions to initiate this chemistry.

We foresee the high modularity of this new donor template giving rise to a diverse assortment of H_2S-releasing compounds by simply changing the nature of the nucleophile and protecting group (Scheme 1). Moreover, in addition to providing a useful set of exploratory tools, we envisage this design strategy to be more likely to harness the therapeutic potential of H_2S by tuning its release to specific conditions where it can provide a pharmacological benefit.

Given the pronounced anti-inflammatory and antioxidative effects of H_2S,[38−40] we were interested in using this chemistry to access a fresh series of thioamide-based donors that were selectively responsive to elevated levels of reactive oxygen species (ROS), providing enhanced spatiotemporal control over their H_2S delivery and fine-tuning their reactivity to conditions where a therapeutic benefit could arise (i.e., protection against cellular oxidative stress).

Although previous ROS-activated, H_2S donors have been reported in the literature,[41−45] these compounds typically undergo a 1,6-elimination to first liberate carbonyl sulfide or COS (another bioactive gas), which is then further converted to H_2S via the enzyme carbonic anhydrase (CA).[46] Furthermore, this reaction pathway leads to the production of a 1,4-quinone methide, which is a highly toxic pro-oxidant that may negate the antioxidative effects of H_2S (Scheme 2a).[47−50]

We proposed that our new donor template could overcome these setbacks by providing the direct liberation of H_2S (as opposed to bioactive COS) under conditions of cellular oxidative stress and via a novel cyclization reaction onto a thioamide that would produce a nontoxic heterocycle as the lone organic byproduct. Moreover, given that similar organic frameworks often serve as privileged scaffolds in medicinal and material chemistry,[51−54] we recognized an interesting and unique opportunity with this template to generate a donor that simultaneously supplies a compound with useful biological and/or chemical properties alongside H_2S.

To this end, in this study, we exploit this innovative chemistry by creating an ROS-activated, self-reporting donor through its concurrent synthesis of a benzoxazole-based fluorophore that coincides with H_2S release (Scheme 2b).

Scheme 2. ROS-Activated H_2S Donors[a]

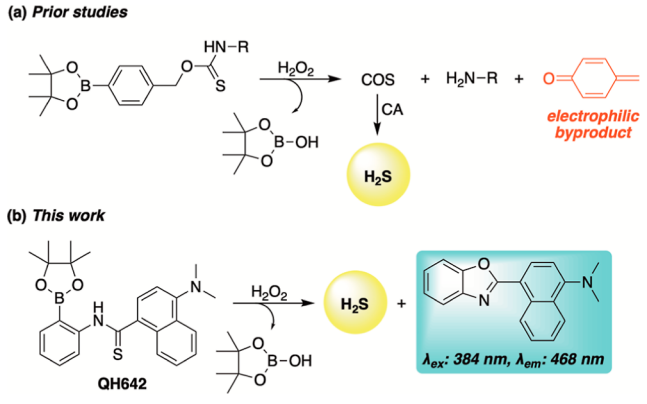

[a](a) Previous efforts that liberate COS, prior to H_2S formation, and alongside a highly electrophilic byproduct. (b) New chemistry describing the direct liberation of H_2S from thioamide-based donors via an oxidation/cyclization pathway. CA = carbonic anhydrase.

RESULTS AND DISCUSSION

Using a boronate ester as a known and highly bioorthogonal reaction partner for hydrogen peroxide (H_2O_2),[55] our studies commenced with the synthesis of compound **1** (Figure 1a).

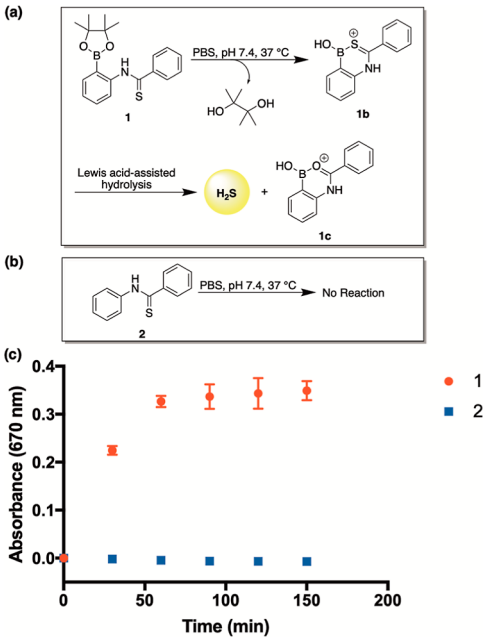

Figure 1. (a) Proposed mechanism for Lewis acid-assisted hydrolysis of **1** (a), but not **2** (b), which facilitates H_2S delivery in buffer at physiological pH. (c) Time-course of H_2S liberation from **1** (50 μM) in 10× PBS (pH 7.4) at 37 °C. For comparison, **2** was tested under identical conditions. Released H_2S was quantified spectrophotometrically using a methylene blue assay (670 nm). Plotted as the mean ± STDEV from three independent experiments.

When compared to our general design strategy depicted in Scheme 1, the nucleophile in **1** is a phenol, protected as a boronate ester to suppress its nucleophilicity. However, in the presence of H_2O_2, we envisioned that boronate ester oxidation would unveil the nucleophilic phenol, which would then cyclize onto the thioamide to assist in H_2S donation.

Before testing this hypothesis, we initially wanted to evaluate the stability of **1** in 10× phosphate-buffered saline (PBS) (pH 7.4) at 37 °C. In our previous studies, we confirmed that most thioamides are robust and resist chemical hydrolysis, even within a complex cellular environment.[37] However, a methylene blue assay, which is a well-established colorimetric method for quantifying the amount of sulfide in solution, indicated that **1** underwent continuous hydrolytic decomposition, releasing approximately 40 μM H_2S (80% yield) within the first hour (Figure 1c). For comparison, we also

https://doi.org/10.1021/jacs.3c10446
J. Am. Chem. Soc. 2023, 145, 25486−25494

examined the stability of control compound **2** (Figure 1b), which lacks the boronate ester. Unlike **1**, compound **2** displayed the hydrolytic stability that we expected from an aryl thioamide as no evidence for sulfide release was observed during the entire 2.5 h incubation period (Figure 1c).

The results of our methylene blue assay were corroborated by LCMS studies, which verified the instability of **1** and its complete conversion to the hydrolyzed amide (**1c**) within 6 h (Figure S1). Conversely, compound **2** displayed excellent stability in buffer and throughout the entire 6 h incubation period with no evidence of amide formation (Figure S2).

Based on this result, we hypothesized that Lewis acid-assisted hydrolysis was likely responsible for the unexpected and rapid decomposition of **1** in buffer (Figure 1a). Intrigued by this result, we next explored the impact of both electronic and steric effects on this hydrolysis pathway by structurally modifying the aryl substituent (R, Figure 2a).

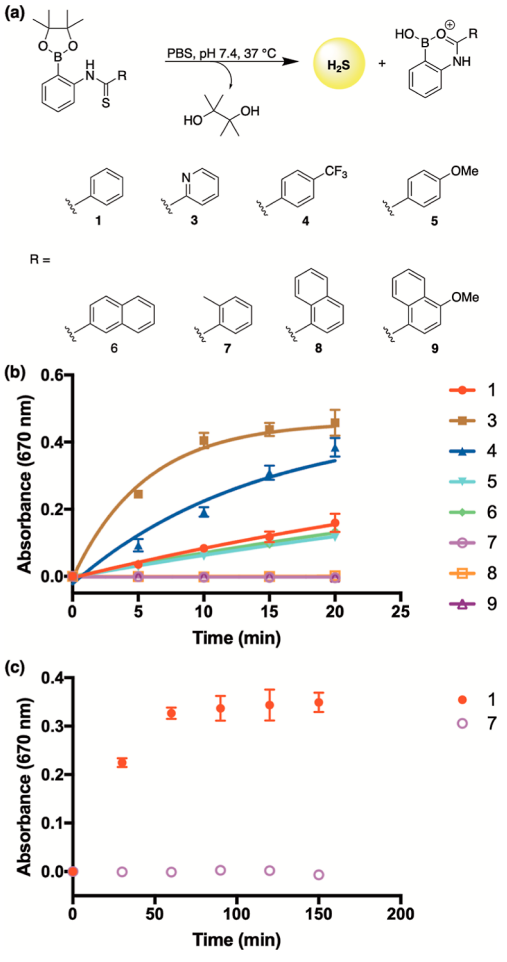

Figure 2. (a) Library of donors tested for Lewis acid-assisted hydrolysis in buffer. (b) Time-course of H_2S liberation from donors (50 μM) in 10× PBS (pH 7.4) at 37 °C. Released H_2S was quantified spectrophotometrically using a methylene blue assay (670 nm). Data points were fit to obtain pseudo-first-order rate constants (k_{obs}): **1**: 0.0210 min^{-1}, **3**: 0.180 min^{-1}, **4**: 0.0715 min^{-1}, **5**: 0.0152 min^{-1}, **6**: 0.0166 min^{-1}, **7**: ND, **8**: ND, **9**: ND. Plotted as the mean ± STDEV from three independent experiments. ND = not determined. (c) Extended time-course to confirm the stability of **7** in 10× PBS (pH7.4 at 37 °C. Released H_2S was quantified spectrophotometrically using a methylene blue assay (670 nm). Plotted as the mean ± STDEV from three independent experiments.

With our library of donors in hand, we monitored their initial rates of H_2S release in buffer by using a methylene blue assay (Figure 2b). As anticipated, a clear trend was observed as the introduction of an electron-withdrawing pyridyl group (**3**) and *para*-trifluoromethyl substituent (**4**) boosted the rates of hydrolysis relative to **1** by more than 8- and 3-fold, respectively. Conversely, but also as expected, compound **5**, which bears an electron-donating *para*-methoxy substituent, was found to be more stable, hydrolyzing at a rate that was about 1.4-fold slower than **1**. Additionally, while the 2-napthyl group (**6**) appeared to have little influence on the rate of hydrolysis relative to **1**, we made the important observation that *ortho*-substituted donors (**7**, **8**, and **9**) appeared to be stable in buffer with no evidence of H_2S release. We speculate that this is due to increased steric effects near the thioamide and (or) a break in conjugation between the aryl ring and thioamide, which significantly suppresses the hydrolytic pathway.

To verify the complete shutdown of Lewis acid-assisted hydrolysis with *ortho*-substituted aryl thioamides, we extended the reaction time of our methylene blue assay. As seen in Figure 2c, throughout the entire time-course, **7**, with an *ortho*-substituted methyl substituent, appeared to be completely stable, with no evidence of sulfide release throughout the entire 150 min incubation. This observation was substantiated by LCMS studies in which a single peak corresponding to the thioamide was observed throughout the entire duration of the experiment (Figure S3).

Having improved hydrolytic stability through *ortho* substitution, we next wanted to assess whether these derivatives could release H_2S in the presence of ROS through a boronate ester oxidation-cyclization pathway, as originally predicted. To test our hypothesis, we exposed **7**, **8**, and **9** (50 μM) to 100 μM H_2O_2 and used a methylene blue assay to measure the amount of sulfide liberated at various time points (Figure 3).

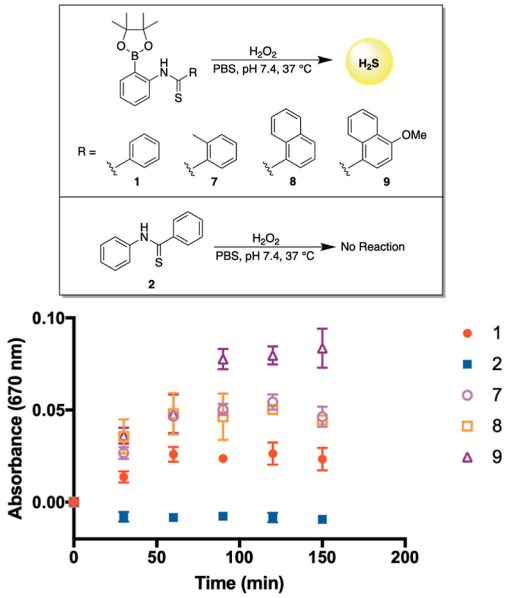

Figure 3. Time-course of H_2S liberation from **1**, **2**, **7**, **8**, and **9** (50 μM) and control compound **2** (50 μM) in 10× PBS (pH 7.4, 37 °C) and in the presence of H_2O_2 (100 μM). Released H_2S was quantified spectrophotometrically using a methylene blue assay (670 nm). Plotted as the mean ± STDEV from three independent experiments.

https://doi.org/10.1021/jacs.3c10446
J. Am. Chem. Soc. 2023, 145, 25486−25494

Scheme 3. Putative Mechanism for H_2S Release from 1 (a) and 7 (b) in the Presence of H_2O_2[a]

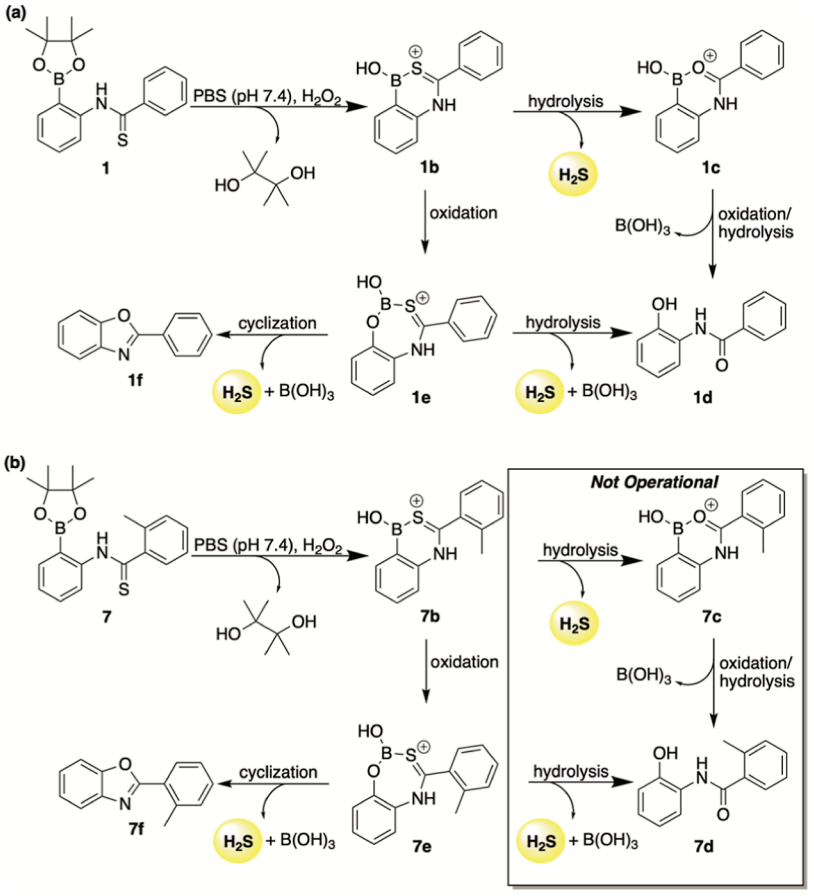

[a]While **1** proceeds through two competing pathways—Lewis acid-assisted hydrolysis and boronate ester oxidation/cyclization—which lead to H_2S delivery, **7** proceeds exclusively through an oxidation/cyclization pathway that liberates H_2S alongside a benzoxazole byproduct (**7f**).

What we observed was that the addition of peroxide does, in fact, stimulate their release of H_2S. For comparison, we also examined **1** and **2** under identical conditions (Figure 3). While control compound **2**, which lacks the boronate ester, appeared to be stable, **1** was found to also donate H_2S upon exposure to peroxide (Figure 3). It is interesting to note that while **7**, **8**, and **9** are completely stable in buffer alone, they appear to release H_2S at a noticeably faster rate than **1** in the presence of H_2O_2. This suggests that while their hydrolytic stability is enhanced, the introduction of an *ortho* substituent might heighten the reactivity of our proposed oxidation/cyclization pathway.

To examine this further, we analyzed the reaction between H_2O_2 and donors **1** and **7** at various time points using LCMS (Figures S4 and S5). The ensuing chromatograms from these studies provided evidence to support the mechanistic pathways that are detailed in Scheme 3 and described below.

In the case of **1** (Scheme 3a), two distinct reaction pathways leading to sulfide delivery were clearly visible. After reacting with peroxide for just 10 min at room temperature, evidence of both Lewis acid-assisted hydrolysis and boronate ester oxidation/cyclization was evident as peaks corresponding to **1c** and **1d**—which follow the Lewis acid-assisted hydrolysis pathway—and **1f**—which is associated with the boronate ester oxidation/cyclization pathway—were observed in the chromatogram (Figure S4). Conversely, donor **7** appears to proceed exclusively through the boronate ester oxidation/cyclization pathway, producing peaks in the chromatogram that correspond to **7e** and **7f**, while being completely devoid of any hydrolysis-related signals, such as **7c** and **7d** (Figure S5). Moreover, while **7e** appears to release H_2S exclusively through a cyclization reaction that produces **7f**, our LCMS studies reveal that H_2S liberation from **1e** also occurs through a hydrolysis pathway that leads to the formation of **1d**. Given the stability of **2** toward hydrolysis, we suspect that this is due to complex **1e**, which is observable by LCMS and likely to promote hydrolysis through Lewis acid assistance. Contrarily, *ortho*-substituted derivatives are stable to hydrolysis and appear to cyclize at a faster rate which converts **7e** exclusively to **7f**.

In total, these studies are highly intriguing as they indicate that the two divergent pathways that lead to H_2S donation can be easily controlled through simple structural modifications that tune the steric and electronic effects of the donor. For example, while donor **1**, which contains a phenyl ring, proceeds through both competing pathways in the presence of H_2O_2 (Scheme 3a), the introduction of an electron-withdrawing group (i.e., pyridyl in place of phenyl) augments the electrophilicity of the thioamide such that it reacts almost entirely via hydrolysis (Figures 2b and S6). On the contrary, *ortho*-substituted donors completely shut down hydrolysis due to steric effects and liberate H_2S exclusively through an oxidation/cyclization pathway (Figures 2b, 3, and S5).

Having tamed this reactivity, we decided to focus our attention on *ortho*-substituted donors, which cleanly afforded

https://doi.org/10.1021/jacs.3c10446
J. Am. Chem. Soc. 2023, 145, 25486−25494

benzoxazole byproducts in response to ROS activation. Given that this molecular framework provides the basis for privileged scaffolds often found in medicinal and material chemistry, we recognized a rare opportunity with this donor class to simultaneously deliver a valuable compound with useful chemical and biological properties alongside H_2S.

From our initial library, we discovered that benzoxazole byproducts derived from **8** and **9** were weakly fluorescent, which is not surprising given the extent of their π conjugation and, in the case of **9**, a slight push−pull effect due to the placement of an electron-donating methoxy group. In an effort to augment the fluorescence properties of the ensuing byproduct, we opted to replace the methoxy substituent on **9** with a more strongly electron-donating dimethylamine (**QH642**, Figure 4a). Indeed, when treated with H_2O_2, **QH642** was found to cleanly provide **DMA-Benzoxa-Fluor** (see Supporting Information), which was found to be slightly red-shifted (ex: 384 nm, em: 468 nm) in terms of its fluorescence (Figure S11).

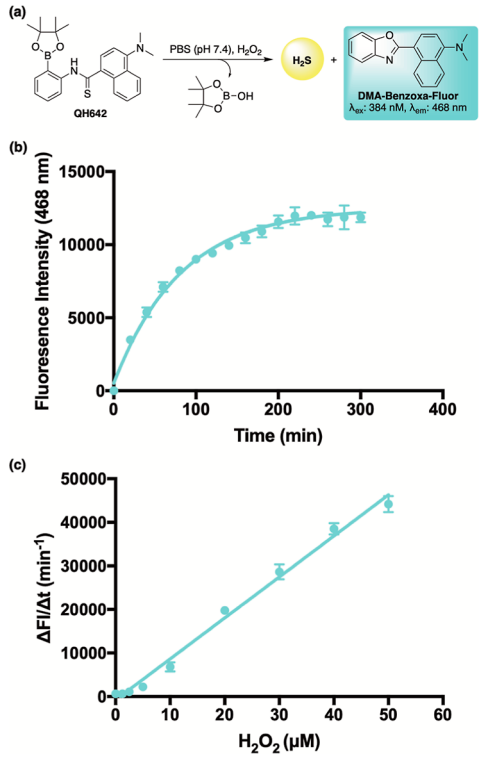

Figure 4. (a) Reaction between **QH642** and H_2O_2 produces a novel benzoxazole-based fluorophore, **DMA-Benzoxa-Fluor**, confirmed by NMR and HRMS (see Supporting Information). (b) Time-dependent fluorescence emission (λ_{ex}: 384 nm, λ_{em}: 468 nm) of **QH642** (10 μM) in PBS (pH 7.4) and in the presence of H_2O_2 (100 μM). Data points were fit to obtain a pseudo-first-order rate constant (k_{obs}) of 0.012 min^{-1} and a half-life of 57 min. Plotted as the mean ± STDEV from three independent experiments. (c) Change in the initial rate of fluorescence intensity of QH642 (10 μM) in the presence of increasing H_2O_2 concentrations. Plotted as the mean ± STDEV from three independent experiments. R^2 = 0.99.

With having what appeared to be a convenient self-reporting system in place, we next examined the reaction between **QH642** (10 μM) and H_2O_2 (100 μM) in 10× PBS (pH 7.4, room temperature) using fluorescence spectroscopy. As illustrated in Figure 4b, we determined that reaction progress could, in fact, be easily gauged by monitoring the fluorescence intensity at the λ_{max} of **DMA-Benzoxa-Fluor** over time. From a calibration curve (Figure S12), it was determined that **DMA-Benzoxa-Fluor** (and therefore H_2S delivery) was afforded at yield greater than 90% after a 5 h incubation period. Importantly, we also verified that the initial response rate ($\Delta FI/\Delta t$) of **QH642** was directly proportional to the concentration of H_2O_2 (Figure 4c). Thus, in addition to monitoring reaction progress, the clean formation of **DMA-Benzoxa-Fluor** endows **QH642** with an ability to function as the H_2O_2 sensor that can be used to not only detect but even quantify the amount of H_2O_2 that is present.

To further validate the delivery of H_2S from **QH642**, we once again employed the colorimetric methylene blue assay (Figure 5a). In the absence of peroxide (10× PBS, pH 7.4, 37 °C), we noted that **QH642** (50 μM) failed to deliver H_2S to any measurable extent, confirming its hydrolytic stability throughout the 2.5 h incubation period. However, with the addition of H_2O_2 (100 μM), a steady increase in absorbance at 670 nm was observed, confirming the release of H_2S from the donor **QH642**.

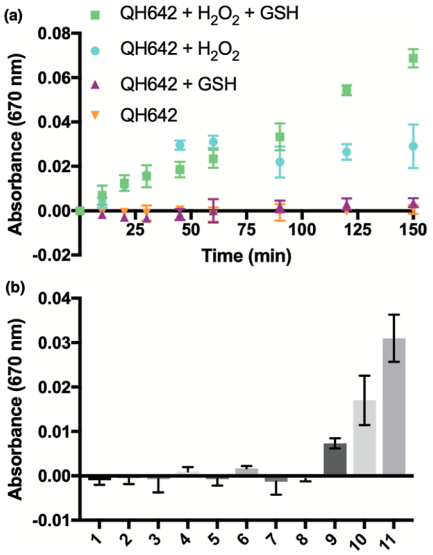

Figure 5. (a) Time-course of H_2S liberation from **QH642** (50 μM) in 10× PBS (pH 7.4, 37 °C) and in either the absence or presence of H_2O_2 (100 μM). To account for sulfide oxidation, in some instances, glutathione (1 mM) was added 5 min prior to the addition of the methylene blue cocktail. Released H_2S was quantified spectrophotometrically using a methylene blue assay (670 nm). Plotted as the mean ± STDEV from three independent experiments. (b) Selectivity of QH642 in 10× PBS (pH 7.4) and in the presence of various biological analytes at 37 °C. (1) PBS alone, (2) 100 μM serine, (3) 100 μM lysine, (4) 1 mM glutathione, (5) 100 μM cysteine, (6) 100 μM homocysteine, (7) 100 μM $NaNO_2$, (8) 100 μM $NaNO_3$, (9) 100 μM KO_2, (10) 100 μM NaOONO, and (11) 100 μM H_2O_2. Released H_2S was determined by using the spectrophotometric methylene blue assay (670 nm). Plotted as the mean ± STDEV from three independent experiments.

Suspecting that the low yield of H_2S (~5 μM based on a calibration curve using Na_2S) was due to a combination of both sulfide and methylene blue oxidation, we repeated the experiment by dousing the reaction mixture with glutathione (1 mM) 5 min prior to the addition of the methylene blue cocktail in an effort to suppress both. Indeed, under these conditions, a noticeable increase in absorbance was recorded,

https://doi.org/10.1021/jacs.3c10446
J. Am. Chem. Soc. 2023, 145, 25486−25494

which corresponded to an H_2S concentration of more than 10 μM being delivered from **QH642**. Still, these results underscore the advantage of a donor with a built-in self-reporting system as monitoring fluorescence and the formation of **DMA-Benzoxa-Fluor** provide a much more accurate depiction of reaction progress.

To ensure that the addition of glutathione was not, by itself, responsible for any H_2S donation, **QH642** was screened against various reductants, nucleophiles, and other oxidants for sulfide release, which confirmed its excellent stability (Figure 5b). However, in addition to H_2O_2, **QH642** was responsive to other ROS, including peroxynitrite and superoxide, consistent with previous reports in the literature.[56]

While data collected from both fluorescence and methylene blue studies inferred that **QH642** was stable to hydrolysis and proceeded exclusively through a boronate ester oxidation/cyclization that formed **DMA-Benzoxa-Fluor** alongside its delivery of H_2S, further validation was obtained by monitoring the reaction between **QH642** and H_2O_2 using LCMS (Figure S7). Similar to *ortho*-substituted donor **7**, the reaction between **QH642 and** H_2O_2 yielded no evidence to support a hydrolysis-related pathway as peaks corresponding **QH642c** and **QH642d** were conspicuously absent from the chromatogram (Figure S7). Instead, unequivocal proof of an oxidation/cyclization pathway was obtained as a peak corresponding to **DMA-Benzoxa-Fluor** was clearly visible and grew steadily over time with the reaction appearing to go cleanly to completion after about 5−6 h, which aligns well with our earlier fluorometer studies (Figure 4b).

As was the case with **1** and **7**, a peak corresponding to the initial oxidized intermediate (**QH642e**, Figure S7) was also observed by LCMS when **QH642** was treated with H_2O_2. We speculated that this Lewis acid complex might facilitate the formation of **DMA-Benzoxa-Fluor** by enhancing the rate of cyclization.

To examine this further, we generated control compound **10** by replacing the boronate ester on **QH642** with a methyl ester (see Supporting Information). With this control compound in hand, the addition of esterase would allow us to compare the rate of cyclization of an analogous phenol that lacks the potential for any Lewis acid assistance. As seen in Figure S9, while the ensuing phenol derived from this key control compound does, in fact, cyclize to produce **DMA-Benzoxa-Fluor**, it appears to do so at a significantly slower rate in both the absence and presence of H_2O_2.

Based on the entirety of our experimental results and control studies, we believe that the following mechanism is likely for the reaction between **QH642** and H_2O_2 (Scheme 4). Upon its addition to buffer, **QH642** rapidly forms a Lewis acid-activated complex (**QH642b**) which is stable to hydrolysis but oxidizes in the presence of H_2O_2 to form **QH642e**. This complex then undergoes a Lewis acid-assisted cyclization that cleanly furnishes **DMA-Benzoxa-Fluor** en route to its release of H_2S.

Finally, we assessed **QH642** within a cellular environment. Given its selective responsiveness toward ROS in buffer (Figure S13), we envisaged its potential to function as a reaction-based sensor for imaging elevated levels of ROS in live human cells.

To test this hypothesis, we first confirmed the low cytotoxicity and high biocompatibility of both **QH642** and **DMA-Benzoxa-Fluor** (Figures S14 and S15). We then verified that **DMA-Benzoxa-Fluor** (40 μM) could be observed intracellularly by confocal fluorescence microscopy (Figure 6a). Once confirmed, we then treated cultured HeLa cells with **QH642** (40 μM) for 1 h prior to imaging. Under these conditions, we did not observe fluorescent cells (Figure 6b). However, when **QH642** was coincubated with H_2O_2 (500 μM), a strong blue fluorescence was observed (Figure 6d), confirming its responsiveness to cellular ROS. As an additional control, HeLa cells were also cotreated with **QH642a** (amide analogue, 40 μM) and H_2O_2 (500 μM) but, as expected, fluorescent cells were not observed (Figure 6c).

We also confirmed the ability of **QH642** to augment the concentration of H_2S in the live HeLa cells. To accomplish

Scheme 4. Putative Mechanism for H_2S Release from QH642 in the Presence of H_2O_2[a]

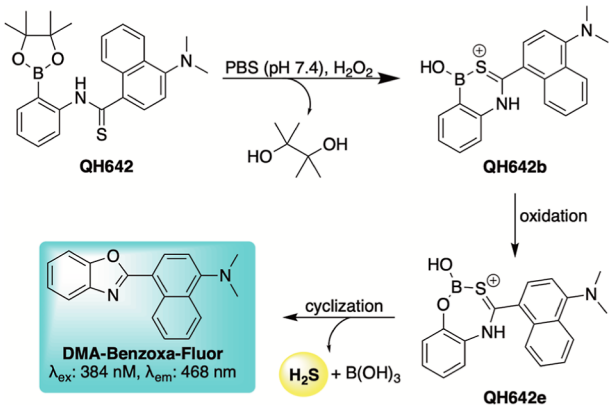

[a]**QH642** resists hydrolysis and proceeds exclusively through an oxidation/cyclization pathway to liberate H_2S alongside a benzoxazole-based fluorophore (**DMA-Benzoxa-Fluor**) which can be used to track reaction progress and verify sulfide delivery.

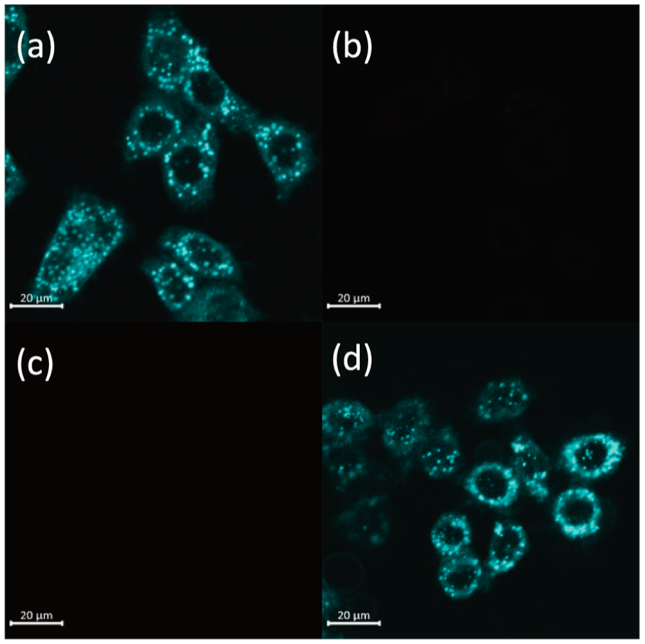

Figure 6. (a) Live HeLa cells stained with **DMA-Benzoxa-Fluor** (40 μM). (b) Live HeLa cells treated with **QH642** (40 μM) for 1 h prior to imaging. (c) Live HeLa cells treated with **QH642a** and H_2O_2 (500 μM) for 1 h prior to imaging. (d) Live HeLa cells treated with **QH642** (40 μM) and H_2O_2 (500 μM) for 1 h prior to imaging. Scale bar was set to 20 μm.

https://doi.org/10.1021/jacs.3c10446
J. Am. Chem. Soc. 2023, 145, 25486−25494

this, cells were first treated with **SS2** (10 μM),[57,58] a reaction-based sensor with high selectivity toward H_2S, followed by the addition of H_2O_2 (500 μM). As seen in Figure 7a, these

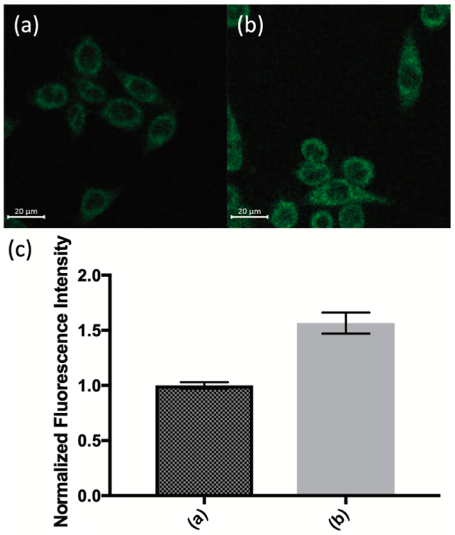

Figure 7. Visualization of the release of H_2S from **QH642** in live HeLa cells. Cells were first treated with SS2 (10 μM) for 1 h. Cells were then washed and treated with either (a) H_2O_2 (500 μM) or (b) H_2O_2 (500 μM) and **QH642** (40 μM). Scale bar was set to 20 μm (c) resulting fluorescence intensity of corresponding cellular images. Values are expressed as the mean ± STDEV over three separate images.

conditions appeared to yield little-to-no fluorescence, presumably due to low levels of endogenous H_2S. However, when **QH642** (40 μM) was added under these same conditions, a noticeable enhancement in green fluorescence was observed (Figure 7b), confirming H_2S delivery from the donor.

Collectively, these results signify that **QH642** has the unique ability to detect and image ROS while simultaneously functioning as an H_2S donor with high biocompatibility and self-reporting capabilities. We believe that these attributes will provide numerous opportunities for **QH642** to serve as a useful bifunctional tool in future cellular studies, which our group is currently pursuing.

CONCLUSIONS

Aryl thioamides flanked with an ortho-substituted boronate ester provide a novel and highly modular platform for H_2S donation. Using this chemistry, a library of donors was accessed and found to release H_2S via two distinct pathways—Lewis acid-facilitated hydrolysis and through an ROS-triggered cyclization. From an extensive structure−activity relationship analysis, we determined that the hydrolysis pathway could be tuned by both steric and electronic effects with less bulky, electron-withdrawing substituents providing the fastest rates of Lewis acid-facilitated hydrolysis. Conversely, we discovered that the hydrolytic pathway could be made completely inoperable with the introduction of ortho-substituents, which forced this donor class to proceed exclusively through an oxidation/cyclization pathway that delivered H_2S directly and selectively in response to ROS. Moreover, we showed that the heterocyclic byproduct that results from this chemistry provides a unique opportunity to generate donors that simultaneously produce compounds with useful biological and chemical properties alongside the delivered H_2S. To highlight this, we also developed an ROS-activated, self-reporting donor (**QH642**) that is likely to find many useful biological applications given its simultaneous synthesis of a novel benzoxazole-based fluorophore (**DMA-Benzoxa-Fluor**) that can be used to monitor reaction progress and H_2S delivery, even within a cellular environment.

ASSOCIATED CONTENT

Supporting Information

The Supporting Information is available free of charge at https://pubs.acs.org/doi/10.1021/jacs.3c10446.

Experimental procedures, characterization data, and NMR spectra (PDF)

AUTHOR INFORMATION

Corresponding Author

John C. Lukesh, III − *Department of Chemistry, Wake Forest University, Winston−Salem, North Carolina 27101, United States;* orcid.org/0000-0001-8436-8491; Email: lukeshjc@wfu.edu

Authors

Qiwei Hu − *Department of Chemistry, Wake Forest University, Winston−Salem, North Carolina 27101, United States*

Changlei Zhu − *Department of Chemistry, Wake Forest University, Winston−Salem, North Carolina 27101, United States*

Rynne A. Hankins − *Department of Chemistry, Wake Forest University, Winston−Salem, North Carolina 27101, United States*

Allison R. Murmello − *Department of Chemistry, Wake Forest University, Winston−Salem, North Carolina 27101, United States*

Glen S. Marrs − *Department of Biology, Wake Forest University, Winston−Salem, North Carolina 27109, United States*

Complete contact information is available at: https://pubs.acs.org/10.1021/jacs.3c10446

Notes

The authors declare no competing financial interest.

ACKNOWLEDGMENTS

We are thankful for financial support from the National Science Foundation (grant no. 2143826).

REFERENCES

(1) Althaus, M.; Clauss, W. G. Gasotransmitters: Novel Regulators of Ion Channels and Transporters. *Front. Physiol.* **2013**, *4*, 1−2.

(2) Papapetropoulos, A.; Foresti, R.; Ferdinandy, P. Pharmacology of the 'Gasotransmitters' NO, CO and H_2S: Translational Opportunities. *Br. J. Pharmacol.* **2015**, *172* (6), 1395−1396.

(3) Wang, R. Shared Signaling Pathways among Gasotransmitters. *Proc. Natl. Acad. Sci. U.S.A.* **2012**, *109* (23), 8801−8802.

(4) Gadalla, M. M.; Snyder, S. H. Hydrogen Sulfide as a Gasotransmitter. *J. Neurochem.* **2010**, *113* (1), 14−26.

(5) Paul, B. D.; Snyder, S. H. H_2S: A Novel Gasotransmitter That Signals by Sulfhydration. *Trends Biochem. Sci.* **2015**, *40* (11), 687−700.

(6) Wang, R. The Gasotransmitter Role of Hydrogen Sulfide. *Antioxid. Redox Signaling* **2003**, *5* (4), 493−501.

(7) Wang, R. Hydrogen Sulfide: The Third Gasotransmitter in Biology and Medicine. *Antioxid. Redox Signaling* **2010**, *12* (9), 1061−1064.
(8) Wang, R. Two's Company, Three's a Crowd: Can H_2S Be the Third Endogenous Gaseous Transmitter? *FASEB J.* **2002**, *16* (13), 1792−1798.
(9) Miles, E. W.; Kraus, J. P. Cystathionine β-Synthase: Structure, Function, Regulation, and Location of Homocystinuria-Causing Mutations. *J. Biol. Chem.* **2004**, *279* (29), 29871−29874.
(10) Pan, L. L.; Liu, X. H.; Gong, Q. H.; Yang, H. B.; Zhu, Y. Z. Role of Cystathionine γ -Lyase/Hydrogen Sulfide Pathway in Cardiovascular Disease: A Novel Therapeutic Strategy? *Antioxid. Redox Signaling* **2012**, *17* (1), 106−118.
(11) Shibuya, N.; Tanaka, M.; Yoshida, M.; Ogasawara, Y.; Togawa, T.; Ishii, K.; Kimura, H. 3-Mercaptopyruvate Sulfurtransferase Produces Hydrogen Sulfide and Bound Sulfane Sulfur in the Brain. *Antioxid. Redox Signaling* **2009**, *11* (4), 703−714.
(12) Abe, K.; Kimura, H. The Possible Role of Hydrogen Sulfide as an Endogenous Neuromodulator. *J. Neurosci.* **1996**, *16* (3), 1066−1071.
(13) Bhatia, M. Hydrogen Sulfide as a Vasodilator. *IUBMB Life* **2005**, *57* (9), 603−606.
(14) White, B. J. O.; Smith, P. A.; Dunn, W. R. Hydrogen Sulphide-Mediated Vasodilatation Involves the Release of Neurotransmitters from Sensory Nerves in Pressurized Mesenteric Small Arteries Isolated from Rats: Hydrogen Sulphide and Vascular Sensory Nerves. *Br. J. Pharmacol.* **2013**, *168* (4), 785−793.
(15) Zhu, X.-Y.; Gu, H.; Ni, X. Hydrogen Sulfide in the Endocrine and Reproductive Systems. *Expert Rev. Clin. Pharmacol.* **2011**, *4* (1), 75−82.
(16) Módis, K.; Ju, Y.; Ahmad, A.; Untereiner, A. A.; Altaany, Z.; Wu, L.; Szabo, C.; Wang, R. S- Sulfhydration of ATP Synthase by Hydrogen Sulfide Stimulates Mitochondrial Bioenergetics. *Pharmacol. Res.* **2016**, *113*, 116−124.
(17) Cao, X.; Cao, L.; Ding, L.; Bian, J. A New Hope for a Devastating Disease: Hydrogen Sulfide in Parkinson's Disease. *Mol. Neurobiol.* **2017**, *55*, 3789−3799.
(18) Giovinazzo, D.; Bursac, B.; Sbodio, J. I.; Nalluru, S.; Vignane, T.; Snowman, A. M.; Albacarys, L. M.; Sedlak, T. W.; Torregrossa, R.; Whiteman, M.; Filipovic, M. R.; Snyder, S. H.; Paul, B. D. Hydrogen Sulfide Is Neuroprotective in Alzheimer's Disease by Sulfhydrating GSK3β and Inhibiting Tau Hyperphosphorylation. *Proc. Natl. Acad. Sci. U.S.A.* **2021**, *118* (4), No. e2017225118.
(19) Murakami, K.; Kato, H.; Hanaki, M.; Monobe, Y.; Akagi, K.; Kawase, T.; Hirose, K.; Irie, K. Synthetic and Biochemical Studies on the Effect of Persulfidation on Disulfide Dimer Models of Amyloid B42 at Position 35 in Alzheimer's Etiology. *RSC Adv.* **2020**, *10* (33), 19506−19512.
(20) Elrod, J. W.; Calvert, J. W.; Morrison, J.; Doeller, J. E.; Kraus, D. W.; Tao, L.; Jiao, X.; Scalia, R.; Kiss, L.; Szabo, C.; Kimura, H.; Chow, C.-W.; Lefer, D. J. Hydrogen Sulfide Attenuates Myocardial Ischemia-Reperfusion Injury by Preservation of Mitochondrial Function. *Proc. Natl. Acad. Sci. U.S.A.* **2007**, *104* (39), 15560−15565.
(21) Johansen, D.; Ytrehus, K.; Baxter, G. F. Exogenous Hydrogen Sulfide (H2S) Protects against Regional Myocardial Ischemia-Reperfusion Injury: Evidence for a Role of KATP Channels. *Basic Res. Cardiol.* **2006**, *101* (1), 53−60.
(22) Li, Z.; Polhemus, D. J.; Lefer, D. J. Evolution of Hydrogen Sulfide Therapeutics to Treat Cardiovascular Disease. *Circ. Res.* **2018**, *123* (5), 590−600.
(23) Piragine, E.; Citi, V.; Lawson, K.; Calderone, V.; Martelli, A. Potential Effects of Natural H2S-Donors in Hypertension Management. *Biomolecules* **2022**, *12* (4), 581.
(24) Sun, W.; Yang, J.; Zhang, Y.; Xi, Y.; Wen, X.; Yuan, D.; Wang, Y.; Wei, C.; Wang, R.; Wu, L.; Li, H.; Xu, C. Exogenous H2S Restores Ischemic Post-Conditioning-Induced Cardioprotection through Inhibiting Endoplasmic Reticulum Stress in the Aged Cardiomyocytes. *Cell Biosci.* **2017**, *7* (1), 67.
(25) Wei, H.; Zhang, R.; Jin, H.; Liu, D.; Tang, X.; Tang, C.; Du, J. Hydrogen Sulfide Attenuates Hyperhomocysteinemia-Induced Cardiomyocytic Endoplasmic Reticulum Stress in Rats. *Antioxid. Redox Signaling* **2010**, *12* (9), 1079−1091.
(26) Wen, Y.-D.; Wang, H.; Zhu, Y.-Z. The Drug Developments of Hydrogen Sulfide on Cardiovascular Disease. *Oxid. Med. Cell. Longev.* **2018**, *2018*, 1−21.
(27) Zhang, Y.; Tang, Z.-H.; Ren, Z.; Qu, S.-L.; Liu, M.-H.; Liu, L.-S.; Jiang, Z.-S. Hydrogen Sulfide, the Next Potent Preventive and Therapeutic Agent in Aging and Age-Associated Diseases. *Mol. Cell. Biol.* **2013**, *33* (6), 1104−1113.
(28) Wilkie, S. E.; Borland, G.; Carter, R. N.; Morton, N. M.; Selman, C. Hydrogen Sulfide in Ageing, Longevity and Disease. *Biochem. J.* **2021**, *478* (19), 3485−3504.
(29) Chemistry, Biochemistry and Pharmacology of Hydrogen Sulfide. In *Handbook of Experimental Pharmacology; Springer International Publishing : Imprint: Springer*, 1st ed.; Moore, P. K., Whiteman, M., Eds.; Springer: Cham, 2015, pp 1−395.
(30) *Hydrogen Sulfide: Chemical Biology Basics, Detection Methods, Therapeutic Applications, and Case Studies*, 1st ed.; Pluth, M., Ed.; John Wiley & Sons, Inc.: Hoboken, NJ, 2023; pp 1−568.
(31) Li, L.; Whiteman, M.; Guan, Y. Y.; Neo, K. L.; Cheng, Y.; Lee, S. W.; Zhao, Y.; Baskar, R.; Tan, C.-H.; Moore, P. K. Characterization of a Novel, Water-Soluble Hydrogen Sulfide-Releasing Molecule (GYY4137): New Insights Into the Biology of Hydrogen Sulfide. *Circulation* **2008**, *117* (18), 2351−2360.
(32) Bora, P.; Chauhan, P.; Pardeshi, K. A.; Chakrapani, H. Small Molecule Generators of Biologically Reactive Sulfur Species. *RSC Adv.* **2018**, *8* (48), 27359−27374.
(33) Hartle, M. D.; Pluth, M. D. A Practical Guide to Working with H_2S at the Interface of Chemistry and Biology. *Chem. Soc. Rev.* **2016**, *45* (22), 6108−6117.
(34) Hu, Q.; Lukesh, J. C. H2S Donors with Cytoprotective Effects in Models of MI/R Injury and Chemotherapy-Induced Cardiotoxicity. *Antioxidants* **2023**, *12* (3), 650.
(35) Levinn, C. M.; Cerda, M. M.; Pluth, M. D. Activatable Small-Molecule Hydrogen Sulfide Donors. *Antioxid. Redox Signaling* **2020**, *32* (2), 96−109.
(36) Xu, S.; Hamsath, A.; Neill, D. L.; Wang, Y.; Yang, C.; Xian, M. Strategies for the Design of Donors and Precursors of Reactive Sulfur Species. *Chem.—Eur. J.* **2019**, *25* (16), 4005−4016.
(37) Hu, Q.; Suarez, S. I.; Hankins, R. A.; Lukesh, J. C. Intramolecular Thiol- and Selenol-Assisted Delivery of Hydrogen Sulfide. *Angew. Chem.* **2022**, *134*, No. e202210754.
(38) Wallace, J. L.; Blackler, R. W.; Chan, M. V.; Da Silva, G. J.; Elsheikh, W.; Flannigan, K. L.; Gamaniek, I.; Manko, A.; Wang, L.; Motta, J.-P.; Buret, A. G. Anti-Inflammatory and Cytoprotective Actions of Hydrogen Sulfide: Translation to Therapeutics. *Antioxid. Redox Signaling* **2015**, *22* (5), 398−410.
(39) Calvert, J. W.; Jha, S.; Gundewar, S.; Elrod, J. W.; Ramachandran, A.; Pattillo, C. B.; Kevil, C. G.; Lefer, D. J. Hydrogen Sulfide Mediates Cardioprotection Through Nrf2 Signaling. *Circ. Res.* **2009**, *105* (4), 365−374.
(40) Xie, Z.-Z.; Liu, Y.; Bian, J.-S. Hydrogen Sulfide and Cellular Redox Homeostasis. *Oxid. Med. Cell. Longev.* **2016**, *2016*, 1−12.
(41) Chauhan, P.; Jos, S.; Chakrapani, H. Reactive Oxygen Species-Triggered Tunable Hydrogen Sulfide Release. *Org. Lett.* **2018**, *20* (13), 3766−3770.
(42) Zhao, Y.; Pluth, M. D. Hydrogen Sulfide Donors Activated by Reactive Oxygen Species. *Angew. Chem.* **2016**, *128* (47), 14858−14862.
(43) Zhu, C.; Suarez, S. I.; Lukesh, J. C. Illuminating and Alleviating Cellular Oxidative Stress with an ROS-Activated, H2S-Donating Theranostic. *Tetrahedron Lett.* **2021**, *69*, 152944.
(44) Powell, C. R.; Dillon, K. M.; Wang, Y.; Carrazzone, R. J.; Matson, J. B. A Persulfide Donor Responsive to Reactive Oxygen Species: Insights into Reactivity and Therapeutic Potential. *Angew. Chem., Int. Ed.* **2018**, *57* (21), 6324−6328.

https://doi.org/10.1021/jacs.3c10446
J. Am. Chem. Soc. 2023, 145, 25486−25494

(45) Hankins, R. A.; Suarez, S. I.; Kalk, M. A.; Green, N. M.; Harty, M. N.; Lukesh, J. C. An Innovative Hydrogen Peroxide-Sensing Scaffold and Insight Towards Its Potential as an ROS-Activated Persulfide Donor. *Angew. Chem., Int. Ed.* **2020**, *59* (49), 22238−22245.
(46) Levinn, C. M.; Cerda, M. M.; Pluth, M. D. Development and Application of Carbonyl Sulfide-Based Donors for H_2S Delivery. *Acc. Chem. Res.* **2019**, *52* (9), 2723−2731.
(47) Monks, T.; Jones, D. The Metabolism and Toxicity of Quinones, Quinonimines, Quinone Methides, and Quinone-Thioethers. *Curr. Drug Metab.* **2002**, *3* (4), 425−438.
(48) Thompson, D. C.; Perera, K.; London, R. Quinone Methide Formation from Para Isomers of Methylphenol (Cresol), Ethylphenol, and Isopropylphenol: Relationship to Toxicity. *Chem. Res. Toxicol.* **1995**, *8* (1), 55−60.
(49) Thompson, D. C.; Thompson, J. A.; Sugumaran, M.; Moldéus, P. Biological and Toxicological Consequences of Quinone Methide Formation. *Chem. Biol. Interact.* **1993**, *86* (2), 129−162.
(50) Pluth, M. D. Moving Past Quinone-Methides: Recent Advances Toward Minimizing Electrophilic Byproducts from COS/H2S Donors. *Curr. Top. Med. Chem.* **2021**, *21* (32), 2882−2889.
(51) Kakkar, S.; Tahlan, S.; Lim, S. M.; Ramasamy, K.; Mani, V.; Shah, S. A. A.; Narasimhan, B. Benzoxazole Derivatives: Design, Synthesis and Biological Evaluation. *Chem. Cent. J.* **2018**, *12* (1), 92.
(52) Law, C. S. W.; Yeong, K. Y. Current Trends of Benzothiazoles in Drug Discovery: A Patent Review (2015−2020). *Expert Opin. Ther. Pat.* **2022**, *32* (3), 299−315.
(53) Reiser, A.; Leyshon, L. J.; Saunders, D.; Mijovic, M. V.; Bright, A.; Bogie, J. Fluorescence of Aromatic Benzoxazole Derivatives. *J. Am. Chem. Soc.* **1972**, *94* (7), 2414−2421.
(54) Das, S.; Indurthi, H. K.; Asati, P.; Saha, P.; Sharma, D. K. Benzothiazole Based Fluorescent Probes for the Detection of Biomolecules, Physiological Conditions, and Ions Responsible for Diseases. *Dyes Pigments* **2022**, *199*, 110074.
(55) Lippert, A. R.; Van de Bittner, G. C.; Chang, C. J. Boronate Oxidation as a Bioorthogonal Reaction Approach for Studying the Chemistry of Hydrogen Peroxide in Living Systems. *Acc. Chem. Res.* **2011**, *44* (9), 793−804.
(56) Zielonka, J.; Sikora, A.; Hardy, M.; Joseph, J.; Dranka, B. P.; Kalyanaraman, B. Boronate Probes as Diagnostic Tools for Real Time Monitoring of Peroxynitrite and Hydroperoxides. *Chem. Res. Toxicol.* **2012**, *25* (9), 1793−1799.
(57) Tian, H.; Qian, J.; Bai, H.; Sun, Q.; Zhang, L.; Zhang, W. Micelle-Induced Multiple Performance Improvement of Fluorescent Probes for H2S Detection. *Anal. Chim. Acta* **2013**, *768*, 136−142.
(58) Choi, S.-A.; Park, C. S.; Kwon, O. S.; Giong, H.-K.; Lee, J.-S.; Ha, T. H.; Lee, C.-S. Structural Effects of Naphthalimide-Based Fluorescent Sensor for Hydrogen Sulfide and Imaging in Live Zebrafish. *Sci. Rep.* **2016**, *6* (1), 26203.

https://doi.org/10.1021/jacs.3c10446
J. Am. Chem. Soc. 2023, 145, 25486−25494